Available online at www.sciencedirect.com
ScienceDirect
Journal of Sound and Vibration 318 (2008) 1313–1333
JOURNAL OF SOUND AND VIBRATION
www.elsevier.com/locate/jsvi

Analysis of handle dynamics-induced errors in hand biodynamic measurements

Ren G. Dong*, Daniel E. Welcome, Thomas W. McDowell, John Z. Wu

Engineering and Control Technology Branch, National Institute for Occupational Safety and Health, 1095 Willowdale Road, Morgantown, WV 26505, USA

Received 24 May 2007; received in revised form 18 April 2008; accepted 21 April 2008
Handling Editor: S. Bolton
Available online 4 June 2008

Abstract

Reliable experimental data of the driving-point biodynamic response (DPBR) of the hand–arm system are required to develop better biodynamic models for several important applications. The objectives of this study are to enhance the understanding of mechanisms of errors induced via the dynamics of instrumented handles and to identify a relatively more reliable method for DPBR measurement. A model of the handle–hand–arm system was developed and applied to examine various measurement methods. Both analytical and finite element methods were used to perform the examinations. This study found that the handle dynamic response could cause an uneven vibration distribution on its structures, especially at high frequencies ($\geqslant 500$ Hz), and hand coupling on the handle could influence the distribution characteristics. Whereas the uneven distribution itself could directly result in measurement error, the hand coupling-induced vibration changes could cause errors in tare mass cancellation. The essential reason for both types of error is that the acceleration measured at one point on the handle may not be the same as that distributed at other locations. Because the cap measurement method that separately measures the DPBRs distributed at the fingers and palm can minimize both types of error, it is the best one among the methods examined in this study. The theory developed in this study can be used to help select, develop, and improve the measurement method for a specific application.
Published by Elsevier Ltd.

1. Introduction

The biodynamics of the hand–arm system is an important part of the foundation for understanding hand-transmitted vibration exposure and its health effects [1,2]. Further advances in biodynamics may play an important role in improving the current vibration exposure assessment standard (ISO 5349-1, 2001) [3]. Recent studies of distributed biodynamic responses have yielded more insight into the characteristics of the biodynamic response [4] and have led to the development of better mechanical-equivalent models for more realistic simulations of the hand and arm structures [5]. Such models have made it possible to provide a reasonable prediction of the vibration power absorbed in the fingers, hand, wrist, arm, and shoulder [6]. These models may lead to an improved understanding of the vibration-induced location-specific disorders [6] and

*Corresponding author. Tel.: +1 304 285 6332; fax: +1 304 285 6265.
E-mail address: rkd6@cdc.gov (R.G. Dong).

0022-460X/$ - see front matter Published by Elsevier Ltd.
doi:10.1016/j.jsv.2008.04.038

discomfort [7]. Whereas these reported models are established based on limited data collected in the z_h-axis (along the forearm axis) [3], more experimental data distributed at the fingers and the palm of the hand are required to verify and improve the biodynamic models.

The driving-point biodynamic response (DPBR) of the hand–arm system is usually expressed as apparent mass or mechanical impedance, and it has been extensively studied [2,8]. However, there are substantial differences among the reported experimental data, especially at high frequencies [9,10]. Some of the reported data are obviously unrealistic [8]. Unfortunately, a portion of the erroneous data was used to synthesize the DPBR values presented in the current ISO 10068 (1998) [11]. The computer models recommended in that standard were also developed based on the questionable DPBR values. Other major problems with the standard include: (i) none of the models recommended provide a reasonable simulation of the anatomical structures of the hand–arm system [12], and (ii) the procedures used to determine the model parameters are questionable, as some of the models do not reasonably fit the experimental data [12]. These observations suggest that ISO 10068 needs major revisions. To facilitate the revisions, a comprehensive understanding of the methods used to measure the reported experimental data is required.

To help achieve this goal, several researchers have conducted some experimental studies and identified several major sources of errors in DPBR measurements (e.g. Ref. [8]). They found that at low frequencies (<25 Hz), significant errors could stem from the phase difference between the acceleration signal and the force signal [8]. If the dynamic forces induced by involuntary hand and arm motions are greater than or comparable with that induced by the vibration excitation, large errors could be observed in the measured data [13]. These errors usually occur in the low frequency range (<10 Hz), because input vibration magnitudes at the low frequencies are usually fairly low. At high frequencies (>100 Hz), major errors could result from inappropriately applied or inaccurate cancellation of the handle mass [8], especially when a time-domain method is used. At any frequency, significant rotational motions of the handle may also result in large measurement errors because the response at one part of the hand could cancel the response of another part of the hand, and the summed response may not provide a reasonable representation of the response in the designed measurement direction.

Although several practical methods have been proposed to identify and resolve the above-mentioned potential problems [8], many phenomena observed in the reported studies have not been sufficiently understood, and some important issues have not been resolved. For example, it is necessary to measure and control the grip force during DPBR measurements, and a split instrumented handle is usually used to measure the grip force (e.g. Refs. [8,14–17]); however, limited studies have been reported as to how the dynamic response of the split handle could affect these measurements [18,19]. Researchers have used different mounting positions for the force sensors used for the dynamic force measurements and for the accelerometers used for vibration measurements; it remains unclear how varying the force and motion transducer locations affects the DPBR results. It is generally believed that the response should be measured at frequencies much lower than the fundamental resonant frequency of the instrumented handle, but the appropriate frequency range remains unknown. Contradicting these generally held beliefs, Dong and his colleagues [8] reported that the DPBR could be measured in the resonant frequency range using their cap measurement method. If this can be theoretically verified, their method can be confidently used for measuring higher frequency DPBRs. They also reported that the hand coupling could significantly reduce the handle's natural frequency along with the resonance magnitude [8]. This brings out a question whether such a change could affect the DPBR measurement. As also observed in the reported studies [8,14,18,19], the handle structures could exhibit some bending motions under vibration. It has not been sufficiently understood exactly how such bending motions could introduce significant measurement error.

The various methods that have been used to measure the DPBR can be roughly classified into two categories: (a) the full handle method [14–17] and (b) the cap method [4]. Traditionally, the response of the entire hand–arm system is usually measured using the first method. Dong and his colleagues [4] initiated the second method, in which the responses distributed at the fingers and the palm of the hand are separately measured, and the total response is obtained by summing the distributed responses. It is unclear which method provides more reliable results. The comparisons of the experimental data in Refs. [4,15] reveal that these two methods generated fairly consistent results at frequencies below 100 Hz, but the trends of their data exhibit

some significant differences at higher frequencies, especially above 500 Hz. It is unclear why there are such large differences.

Based on this background, the specific aims of this study were to understand the exact mechanisms of the handle dynamics-induced errors and to examine these two groups of DPBR measurement methods so that a relatively more reliable method could be identified. A model of a typical instrumented handle was developed. Together with a recently reported hand–arm system model [5], the handle model was used to examine the detailed mechanisms of errors induced from dynamics of the handle structures and to evaluate these measurement methods. Based on the results of the analyses and simulations, the above-mentioned issues or questions were discussed. As a result, a general principle for accurately measuring the DPBR was proposed, and the most reliable method was identified.

2. Methods

2.1. System model

Fig. 1 shows the four-degrees-of-freedom model of the hand–arm system reported recently [5]; its parameters are listed in Table 1. The DPBR predicted by this model agree very well with the reported experimental data [4]. In this model, the apparent mass distributed at the fingers (M_{Fingers}), that at the palm (M_{Palm}), and the total response (M_{Hand}) are expressed as follows [5]:

$$\begin{aligned} M_{\text{Fingers}} &= F_4/A_{\text{Fingers}} + M_4 \\ M_{\text{Palm}} &= F_3/A_{\text{Palm}} + M_3 \\ M_{\text{Hand}} &= M_{\text{Fingers}} + M_{\text{Palm}} \end{aligned} \tag{1}$$

where F_3 is the complex force acting on K_3 and C_3; F_4 is that acting on K_4 and C_4; A_{Fingers} is the acceleration input to the fingers; A_{Palm} is that input to the palm. A_{Fingers} and A_{Palm} are the same if the handle is considered as a rigid body. For the purpose of this study, the responses directly calculated using these formulas are termed as the 'accurate solution'; these values are used in comparisons with those from the simulations of the various measurement methods.

Fig. 2 shows a measurement system used for measuring the driving-point biodynamic response of the hand–arm system exposed to vibration in one direction [4]. The instrumented handle is fixed on the handle fixture that is installed on the shaker. The handle is composed of a measuring cap, a handle base, two force sensors sandwiched between the measuring cap and the base, and an accelerometer fixed on the measuring cap.

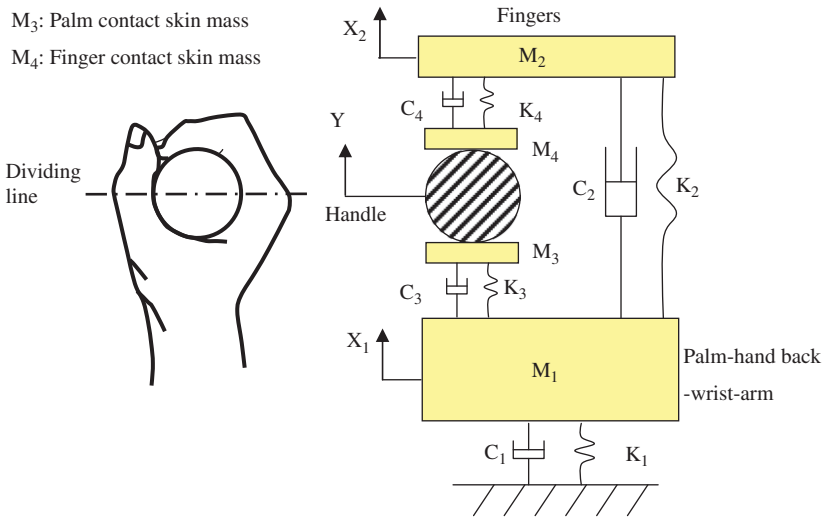

Fig. 1. A four-degrees-of-freedom model of the hand–arm system [5].

Table 1
Parameters of the hand–arm system model [5]

Parameter	Value (kg)	Parameter	Value (N/m)	Parameter	Value (N s/m)
M_1	1.414	K_1	4206	C_1	86
M_2	0.082	K_2	6523	C_2	38
M_3	0.027	K_3	58,555	C_3	118
M_4	0.014	K_4	207,964	C_4	121

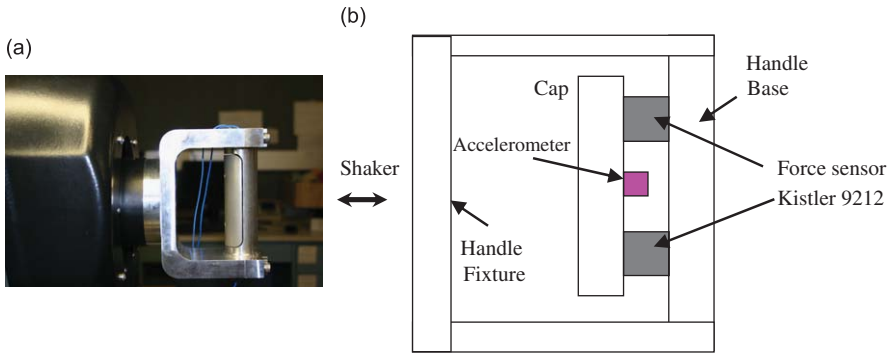

Fig. 2. A device used to measure the biodynamic response of hand–arm system [4]: (a) a pictorial view of the device; and (b) configurations of instrumented handle.

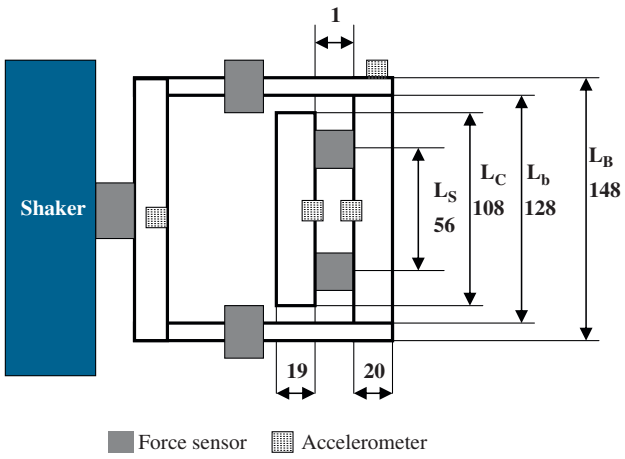

Fig. 3. Handle dimensions (in mm) and possible positions of the force and motion sensors for the DPBR measurement.

The handle is fixed on the handle fixture that is connected to a shaker. This measurement system was used as the basis for the modeling analysis.

Fig. 3 shows various sensor positions that have been used in the reported studies [8,14–17]. Based on these sensor positions, the instrumented handle was modeled using the structure shown in Fig. 4. Assembling the hand–arm system model into the instrumented handle model, a model of the entire handle–hand–arm system was formed and it is illustrated in Fig. 5.

2.2. Modeling with a finite element method

As the first approach, a finite element method was used to perform the modeling analysis. Whereas the measuring cap was modeled as a uniform Euler–Bernoulli beam, the handle base was modeled as a staged

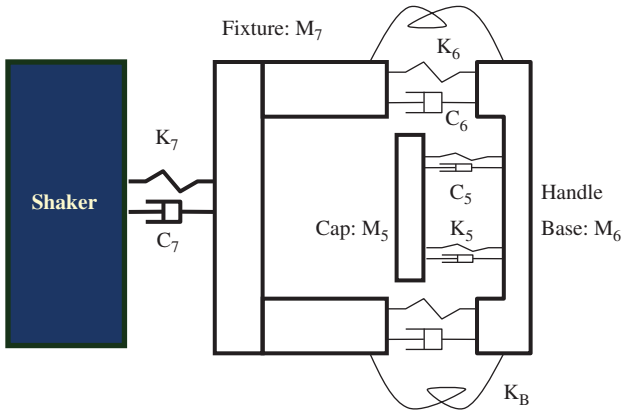

Fig. 4. A model of the instrumented handle: the measuring cap as a uniform Euler–Bernoulli beam; the handle base as a staged Euler–Bernoulli beam, the handle fixture as a rigid body; they are connected with linear spring-damper elements.

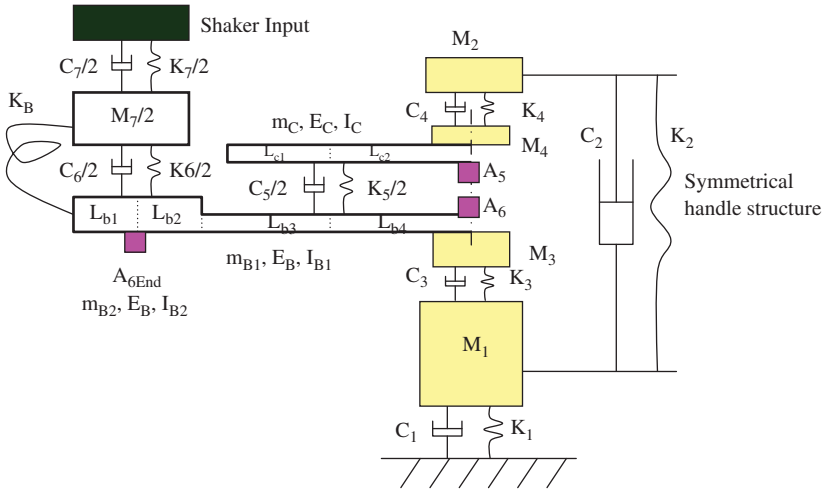

Fig. 5. A model of the measurement device coupled with a hand–arm system.

Euler–Bernoulli beam. The cap was divided into four beam finite elements, and the base was divided into eight beam finite elements, which are also illustrated in Fig. 5. The finite element formulas described in Ref. [20] were used to simulate each beam element. The force sensors were represented using linear spring and viscous damping elements. A bending spring element was also considered at each connection between the fixture and the handle base. Half of the mass of each force sensor was lumped to each end of the corresponding spring-damper element rigidly connected to a node of the corresponding beam element. Whenever applicable, the mass of the accelerometer was lumped to the rigid body element or the node of the finite element where the accelerometer was positioned.

In this study, the inputs from the shaker to the handle at the two fixture-handle connection points were assumed to be the same. Therefore, only the symmetric bending modes of the handle cap and base were simulated in this study. Whereas the essential dimensional parameters of the fixture-handle model are provided in Fig. 4, the baseline parameters of this model are summarized in Table 2. Unless specified otherwise, these parameters were used in the modeling analysis. The geometric parameters of the handle cap and base beams were obtained from their technical drawings. Their material properties were gleaned from a handbook [21]. The stiffness between the shaker and the fixture (K_7) and that between the handle and handle fixture (K_6) on the measurement system shown in Fig. 2 must be very high, but it is very difficult to measure

Table 2
Baseline parameters of the fixture and handle

Parameter	Value	Parameter	Value	Parameter	Value
Lumped parameters					
M_5 (kg)	0.105	K_5 (kN/m)	12,880	C_5 (N s/m)	60
M_6 (kg)	0.269	K_6 (kN/m)	57,000	C_6 (N s/m)	60
M_7 (kg)	1.200	K_7 (kN/m)	500,000	C_7 (N s/m)	100
Accelerometer mass (kg)	0.005	K_B (kN m/rad)	100	Force sensor mass (kg)	0.022
Cap beam properties and finite element meshing					
Magnesium:					
m_C (kg/m)	0.725	E_C (N/m^2)	4.5e10	I_C (m^4)	1.742e−8
L_{c1} (m)	0.026	L_{c2} (m)	0.028		
Base beam properties and finite element meshing					
Aluminum:					
m_{B1} (kg/m)	1.148	E_B (N/m^2)	7.2e10	I_{B1} (m^4)	1.759e−8
m_{B2} (kg/m)	2.56			I_{B2} (m^4)	1.18e−7
L_{b1} (m)	0.010	L_{b2} (m)	0.011		
L_{b3} (m)	0.025	L_{b4} (m)	0.028		

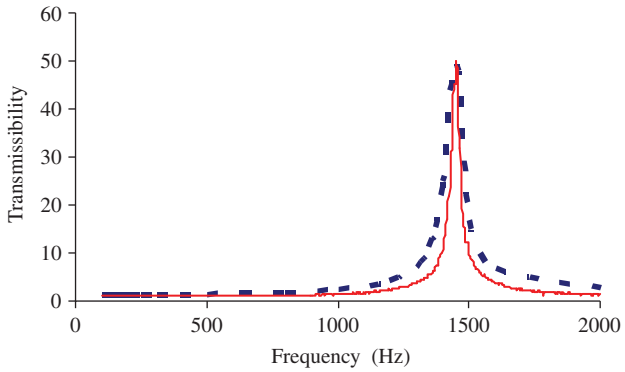

Fig. 6. Comparison of vibration transmissibility response (relative to handle fixture) measured on the measuring cap (————) [8] and that predicted using the model (- - - - - -).

them. To evaluate the uncertainty of these parameters, a parametric study was performed on the modeling results to assess the effects of their variations on the DPBR prediction. The reported experimental study found that the major relative displacement in the handle structures was at the force sensor connection between the cap and the base [8]. Therefore, the stiffness and damping at this location (K_5 and C_5) were determined by matching the frequency response measured on the measuring cap [8] with that predicted using the handle model (without the hand coupled to the handle). The matching results are shown in Fig. 6. A parametric study was also performed to evaluate the variations of the stiffness and damping at this location and its effects on the DPBR measurement.

The equations of motion of the entire system subjected to shaker sinusoidal excitation $y(t)$ are expressed in the matrix form as

$$\mathbf{M}\cdot\ddot{\mathbf{q}}+\mathbf{C}\cdot\dot{\mathbf{q}}+\mathbf{K}\cdot\mathbf{q}=\mathbf{f}, \tag{2}$$

where $\mathbf{M}$ is the mass matrix, $\mathbf{C}$ is the damping matrix, $\mathbf{K}$ is the stiffness matrix, $\mathbf{f}$ is the force vector, and $\mathbf{q}$ represents the vector response coordinates.

The equations of motion were solved to derive biodynamic forces acting at the connection points and the accelerations of mass elements of the model. Then, the apparent mass (M_{ik}) was calculated using the force at

the ith point (F_i) and the acceleration of the kth part (A_k) from:

$$M_{ik}(\mathrm{j}\omega) = F_i(\mathrm{j}\omega)/A_k(\mathrm{j}\omega), \tag{3}$$

where $\mathrm{j} = \sqrt{-1}$, and ω is the excitation frequency. The mechanical impedance (Z_{ik}) was further calculated from

$$Z_{ik}(\mathrm{j}\omega) = M_{ik}(\mathrm{j}\omega)\mathrm{j}\omega. \tag{4}$$

2.2.1. Simulation of the cap measurement method

The cap measurement method reported in Ref. [4] was simulated in this study. This method measures the finger DPBR or the response distributed at the fingers when the fingers are positioned on the measuring cap, and it measures palm DPBR when the palm is positioned on the measuring cap. Then, the superposition of the finger DPBR and palm DPBR is taken as the DPBR of the entire hand–arm system or the hand DPBR, as expressed in Eq. (1). Specifically, the finger DPBR measurement was simulated using the exact model shown in Fig. 5. The palm DPBR measurement was simulated by rotating the hand–arm system model 180° around the handle longitudinal axis such that M_3 is positioned on the measuring cap and M_4 is positioned on the handle base. In each case, DPBR is evaluated using the acceleration measured on the measuring cap (A_5) and the dynamic force (F_5) measured using the two force sensors sandwiched between the cap and the handle base, which are represented using K_5 and C_5 in the model shown in Fig. 5. The tare mass of the measurement system was cancelled using the frequency domain method described in Ref. [4], which is expressed as follows:

$$M_{\mathrm{Fingers\_or\_Palm}}(\mathrm{j}\omega) = M_{\mathrm{FCoupled}}(\mathrm{j}\omega) - M_{\mathrm{Cap}}(\mathrm{j}\omega), \tag{5}$$

where M_{FCoupled} is the total response of the cap and the fingers or the palm–wrist–arm system when the hand is coupled to the handle, and M_{Cap} is the tare mass response of the cap assembly without hand coupling.

Theoretically, any difference between the accurate solution expressed in Eq. (1) and that calculated using Eq. (5) reflects the influence of the handle structure responses on the DPBR measurement. The difference was thus considered as the error of the measurement method simulated in this study. This concept also applies to the full handle measurement method.

2.2.2. Simulation of the full handle measurement methods

The specific handle structures used in the measurement of the DPBR of the entire hand–arm system may vary greatly among the reported studies. For example, in one study, unlike the handle structure shown in Fig. 2, two caps are connected to the two parallel handle base beams that are in turn connected to the handle fixture [10]. In another example, the two force sensors are fixed on the handle fixture [17]. Whereas it is difficult to simulate all the detailed handle structures used in the reported studies, the model shown in Fig. 5 was used as the basis to analyze the basic measurement principles of these methods and to understand the mechanisms of the handle tare structure effects on DPBR measurements.

Similar to the cap method, the force measured on the two sensors connecting the handle cap and base (F_5) was generally used to quantify the applied grip force in the full handle methods (e.g. Ref. [15]). Some of the methods used strain gauges installed on the cap and/or base beams to detect the grip force (e.g. Refs. [16,17]). The dynamic force distributed at the two force sensors at the handle–fixture connections (F_6) (e.g. Refs. [15,17]) or at the fixture-shaker armature connection (F_7) (e.g. Ref. [16]) was measured and used to evaluate the DPBR of the entire hand–arm system. The acceleration required in the evaluation was measured either on the impedance head (or fixture) (e.g. Ref. [16]), or the handle base (e.g. Ref. [15]), or the measuring cap (e.g. Refs. [10,17]). The various combinations of the force and motion measurements for the DPBR evaluation were simulated in the current study.

Similar to the procedure used in the simulation of the cap measurement method, the tare mass of the handle assembly was cancelled using the following formula:

$$M_{\mathrm{Hand}}(\mathrm{j}\omega) = M_{\mathrm{HCoupled}}(\omega) - M_{\mathrm{Handle}}(\omega), \tag{6}$$

where M_{HCoupled} is the response of the entire handle–hand–arm system, and M_{Handle} is the handle's mass response without hand coupling.

The finite element modeling was programmed using both MS Excel and Matlab. The two programs produced identical solutions.

2.3. Analytical method

In addition to the finite element method, this study also proposed an analytical method and applied it to examine various DPBR measurement methods. The analytical solutions were obtained in three steps. As the first step, the measuring cap and handle base in the system model shown in Fig. 5 were simplified as two rigid bodies, M_5 and M_6, respectively. The solutions were expressed in analytical formulas that were derived using the simplified model, together with Eqs. (1) (3), (5) and (6). As the second step, the effects of the bending motion on the DPBR measurement were examined. The analytical formulas were derived using the conceptual models shown in Fig. 7 along with Eqs. (1), (3), (5) and (6). Finally, the solution for each typical DPBR measurement method was obtained by superimposing the separate solutions obtained in the first two steps. The detailed analytical method and solutions are presented in Appendix A.

The combination of the analytical method and the finite element method provides a powerful approach to understand the handle dynamics-induced DPBR measurement errors. Whereas the analytical formulas provide the general concept on the mechanism of the error generation, the finite element solutions provide the specific values for assessing the significance of the error at each frequency. While the numerical solutions reflect the combined effect of the influencing factors involved in the DPBR measurement, the analytical formulas were used to identify the general role of each essential factor in the error generation. The analytical solutions and the finite element results were also used to verify each other in this study. Therefore, their solutions are presented jointly in the following section.

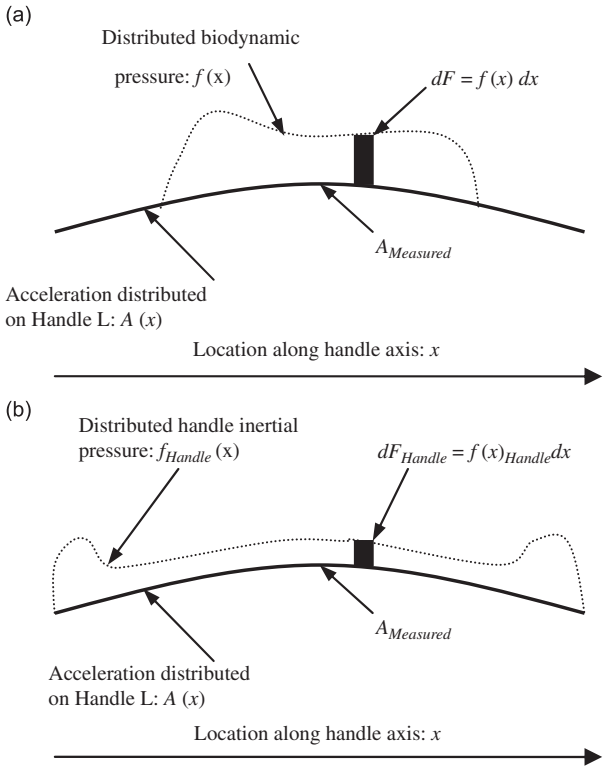

Fig. 7. Conceptual models for assessing the effects of handle bending motion on the biodynamic response measurement and handle tare mass cancellation: (a) biodynamic force distribution; and (b) handle inertial force distribution.

3. Results

3.1. Handle structure vibration modes and hand coupling effects

Fig. 8 shows the cap vibration transmissibility function predicted using the finite element model shown in Fig. 5, together with the experimental data reported in Ref. [8]. The comparison of the experimental and modeling data suggests that the proposed model provided a reasonable prediction of the measuring cap response. Both the modeling results and the experimental data show that the hand coupling substantially reduces the resonant peak from that without hand coupling shown in Fig. 6. These results also show that the coupling reduces the handle resonant frequency. The differences between the transmissibility values shown in Figs. 6 and 8 indicate that hand coupling could increase vibration magnitudes at frequencies below approximately 1300 Hz while reducing vibration magnitudes at higher frequencies.

Fig. 9 shows the predicted accelerations distributed on the cap and base along the axis of the 40 mm handle with and without hand coupling at three frequencies (1000, 1250, and 1600 Hz). In these examples, the given acceleration input from M_7 to the handle base in Fig. 5 is 10 m/s^2 at each frequency. The vibration on the cap at each location and each frequency is different from that on the base. Most of this vibration variation results from differences in the rigid body vibration modes of these two structures, which is termed as inter-structure vibration variation in this study. Superimposed on the rigid body mode, the remaining difference results from the bending motion of each structure, which is termed as intra-structure vibration variation. The relative bending motion on the cap is generally less than that on the handle base. As also shown in Fig. 9, hand coupling significantly affected both inter- and intra-structure motions. Also consistent with that observed in Figs. 6 and 8, hand coupling reduced the magnitude of vibration at 1600 Hz, but it increased vibration magnitude at other two frequencies.

3.2. The cap measurement method

Fig. 10 shows the mechanical impedance functions of the fingers predicted via the finite element modeling, together with the accurate solution. Although the measuring cap responds differently with and without hand coupling, the impedance phase evaluated using F_5 and A_5 is almost identical to the accurate solution in the entire frequency range of concern ($\leqslant$2000 Hz) in this study. Generally, there is more underestimation as frequency increases, but this error is less than 5% up to 1500 Hz and less than 7.8% up to 2000 Hz. The cap's resonance in the range of 1300 to 1500 Hz, shown in Figs. 6 and 7, has little effect on the BR measurement. When the hand was assumed to be fully positioned on the cap over the force sensors, little error at any frequency was observed. At the cap end (extreme condition), the DPBR was overestimated by less than 10% up to 1500 Hz. Considering that the hand contact area is generally near and between the two force sensors in the experiment [4], these modeling results suggest that the overall potential error is less than $\pm$5% at frequencies up to 1500 Hz.

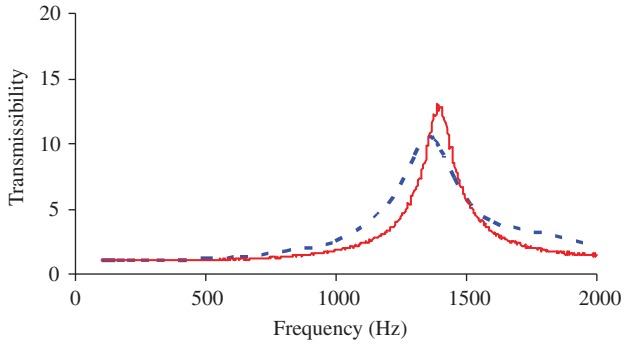

Fig. 8. Effect of the hand coupling on the vibration transmissibility response (relative to handle fixture): (————), experimental data reported in Ref. [8]; and (- - - - - -), predicted from the modeling.

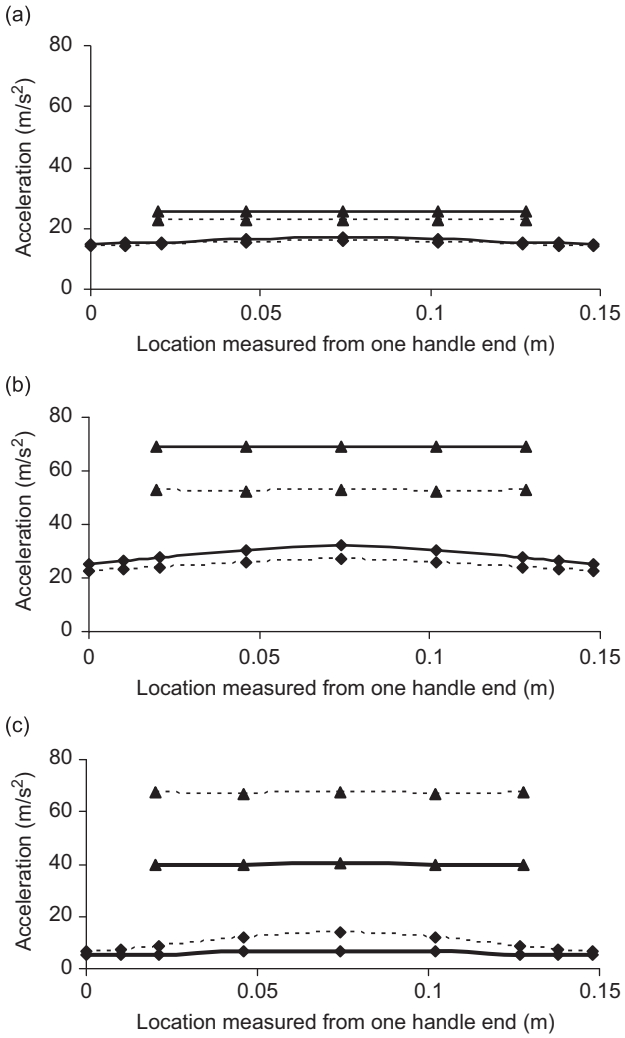

Fig. 9. Predicted acceleration distributions on the measuring cap and base along the handle's longitudinal axis with and without hand coupling: (a) 1000 Hz; (b) 1250 Hz; and (c) 1600 Hz. ((—▲—), cap with hand coupling; (···▲···), cap without hand coupling; (—◆—), base with hand coupling; and (···◆···), base without hand coupling).

Fig. 10 also shows that when F_5 and the acceleration on the handle base (A_6) are used in the evaluation, the impedance magnitude is greatly overestimated at frequencies above 250 Hz, whereas the impedance phase is underestimated.

The analytical solutions presented in Appendix A indicate that the DPBR measured using the cap method is accurate when the handle cap is considered as a rigid body. The solution is independent of the instrumented handle's mass, stiffness, and damping parameters. Only the cap's bending could affect the solution. These observations are consistent with the above-presented finite element results.

Several parametric studies using the finite element model were performed to identify and examine the effect of the handle mechanical properties on the finger DPBR evaluation. The connection parameters K_5, C_5, K_6, C_6, and K_B were varied from 1/20 to 20 times their baseline values listed in Table 2. Such large variations in these parameters produce less than 2.5% variations in the calculated responses. The handle base and cap may be softer than they are in the model because the Euler–Bernoulli beam does not take into account the shear deformation and rotational inertia of the handle structures. The holes in the base and cap for the installations of the sensors must also weaken these structures, but it is difficult to directly simulate them in the modeling. Alternatively, these stiffness-softening factors were qualitatively taken into account by reducing the Young's

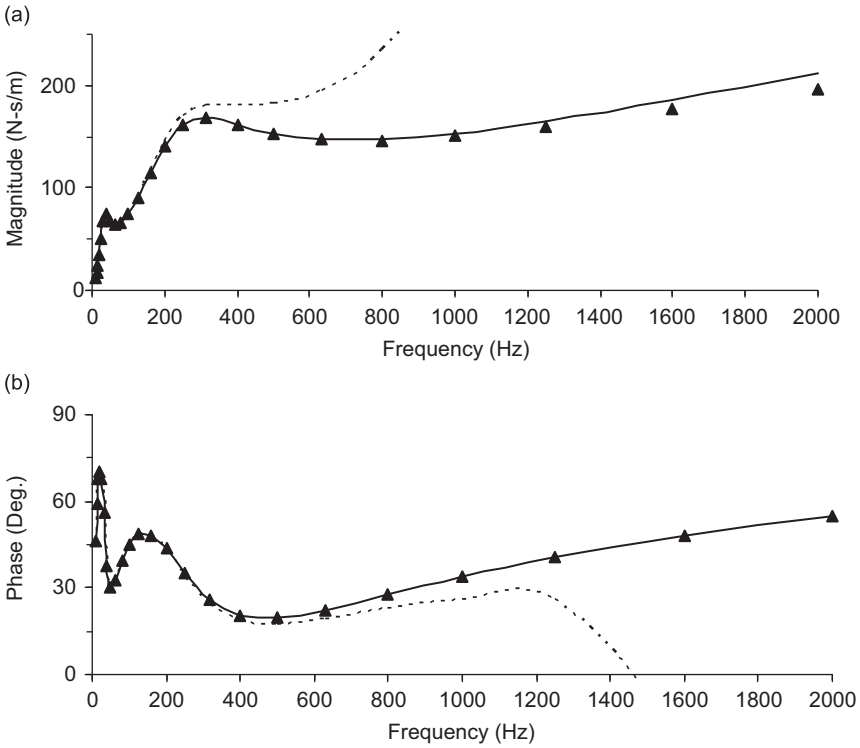

Fig. 10. Mechanical impedance distributed at the fingers: (a) magnitude; and (b) phase. (_____, accurate solution; ▲, evaluated using F_5 and A_5; and ·····, evaluated using F_5 and A_6).

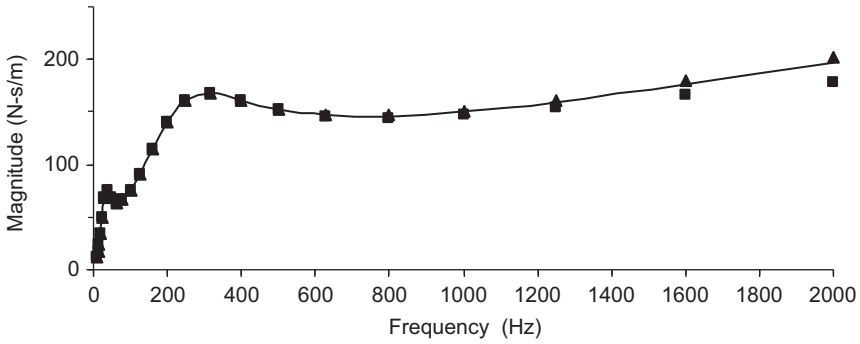

Fig. 11. Effect of the measuring cap stiffness on the magnitude of finger impedance (■, 0.5 E_c; _____, E_c; ▲, 1.5 E_c).

modulus of the handle base or the cap. The reduction of the handle base modulus was as much as five times the baseline value listed in Table 2, but it had little effect on the finger DPBR. However, when the measuring cap was softened, the DPBR magnitude decreased with the reduction in the cap modulus or stiffness, as shown in Fig. 11. Fortunately, the effect is not sensitive because a one-half reduction in cap stiffness only reduced the DPBR by less than 10% at frequencies up to 1500 Hz.

The palm was positioned on the measuring cap and the fingers on the handle base to simulate the palm response measurement using the cap method [4]. Fig. 12 shows the comparison of the accurate solution and that generated from the modeling for the response distributed at the palm of the hand. The basic phenomena were the same as those observed in the simulations of the response distributed at the fingers. Therefore, the total hand–arm system responses summed from the responses distributed at the fingers and the palm evaluated

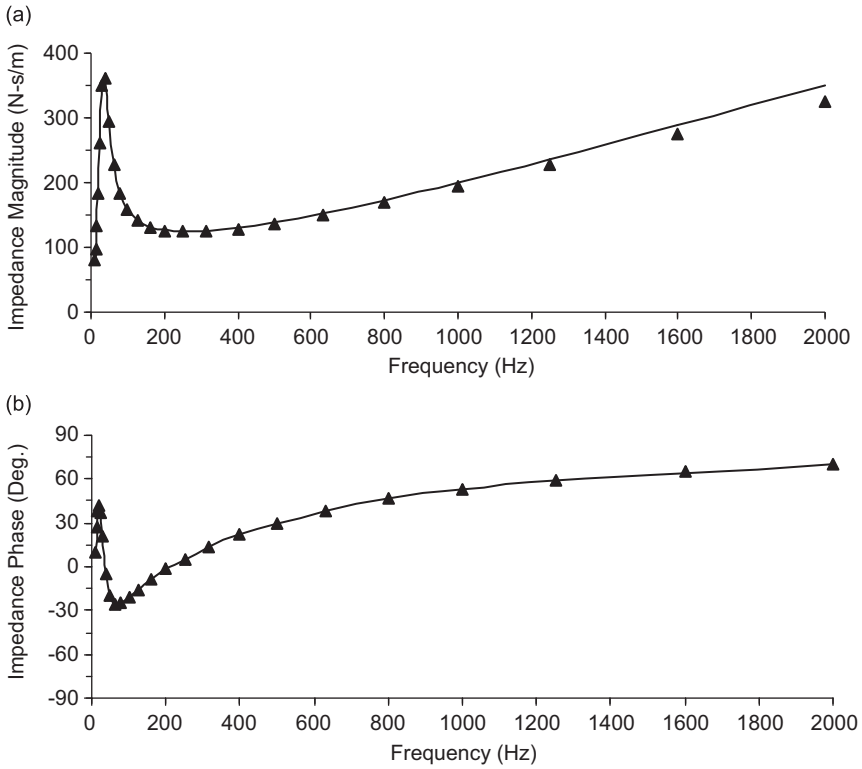

Fig. 12. Mechanical impedance distributed at the palm: (a) magnitude; and (b) phase. (_____, accurate solution; and ▲, evaluated using F_5 and A_5).

using F_5 and A_5 were also very close to the accurate solution (less than $\pm 5\%$ error at frequencies up to 1500 Hz).

In the handle operational calibration test or check-up test [8], a rigid mass was firmly attached to the measuring cap. This test was simulated by replacing the hand–arm system model with a single mass. In the modeling, the calibration mass was positioned at three locations: at the cap center, on the cap over one of the force sensors, and at the end of the cap. As observed above, the error generally increased with the increase in frequency. The percent error also varied with the location and the mass value. For example, at 2000 Hz, the error for a 20 g mass was -0.23% when positioned over the force sensor, -7.70% at the cap center, and $+22.60\%$ at the cap end. The check-up mass in the range of 5–50 g had little effect on the error when positioned over the force sensor or at the cap center, but the variation had some influence on the result when positioned at the cap end. For example, at 1000 Hz, the errors at the cap end were $+3.72\%$ and $+8.07\%$ for 5 and 50 g calibration masses, respectively. At 2000 Hz, they were $+15.69\%$ and $+39.24\%$, respectively.

3.3. The full handle measurement methods

Different from the cap method, a full handle method with a split handle is generally influenced by both inter- and intra-structure vibration variations. Because the first resonance of the measuring cap is primarily resulted from the flexibility of the cap-base connection on the 40 mm handle used in this study, the inter-structure vibration variation plays a dominant role in influencing the full hand DPBR measurement. Its influence can be understood by applying the analytical formulas derived under the assumption that the measuring cap and handle base are rigid bodies. For example, the DPBR (M_{66}) of the hand–arm system evaluated with the acceleration on the handle base (A_6) and the dynamic force (F_6) represented using K_6 and

C_6 can be expressed as follows (see Appendix A for more details):

$$M_{66} = M_{\text{Palm}} + \alpha M_{\text{Fingers}} + (\alpha - \beta)M_5 \neq M_{\text{Hand}}, \tag{7}$$

where

$$\alpha = A_{5\_\text{Coupled}}/A_{6\_\text{Coupled}},$$
$$\beta = A_{5\_\text{Uncoupled}}/A_{6\_\text{Uncoupled}}, \tag{8}$$

where "Coupled" and "Uncoupled" refer to the measurement with and without hand coupling, respectively.

Eq. (7) indicates that, similar to the use of F_5 and A_5 for simulating the cap method, the use of F_6 and A_6 can provide accurate measurements for the DPBR distributed at the palm if the base bending effect can be ignored. However, this equation also includes two error terms that involve two independent variables: α-value and β-value. The first error term reflects the effect of the inter-structure (cap vs. base) vibration difference, represented by α-value, on the finger DPBR measurement (M_{Fingers}). The second error term, represented by the $(\alpha-\beta)$-value, reflects the hand coupling effect on the tare mass (M_5) cancellation.

Because the inter-structure vibration variation plays a dominant role in this case, the transmissibility shown in Fig. 6 primarily represents the β-value and that in Fig. 8 primarily represents the α-value. Because both α and β-values are very close to unity at frequencies less than 200 Hz, Eq. (7) predicts that M_{66} is approximately equal to M_{Hand} at such frequencies. However, the transmissibility values suggest that DPBR errors could generally increase with the increase in frequency. Because the α-value is greater than one in the entire frequency range of concern, the first type of error results in an overestimation of the DPBR. Because the α-value is greater than the β-value at frequencies less than 1300 Hz, as shown in Fig. 7, the second type of error also results in an overestimation of the DPBR in such a frequency range. On the other hand, if F_6 and A_5 are used for DPBR evaluation, these two types of error could result in an underestimation of the full hand DPBR at such frequencies because it can be expressed as follows:

$$M_{65} = M_{\text{Fingers}} + \frac{1}{\alpha}M_{\text{Palm}} + \left(\frac{1}{\alpha} - \frac{1}{\beta}\right)M_6 \neq M_{\text{Hand}}. \tag{9}$$

The specific error values at each frequency were predicted via finite element modeling. Fig. 13 shows the calculated numerical solutions for the mechanical impedances of the entire hand–arm system using the force (F_6) acting on K_6 and C_6 and the accelerations at four locations. The accurate solution is also displayed in the figure. Consistent with the analytical predictions, the errors for each DPBR measurement method are generally less than 5% at frequencies lower than 200 Hz. The errors for each method generally increase with the increase in frequency. Whereas the use of the acceleration on the measuring cap (A_5) underestimates the DPBR, the use of the accelerations at other three locations (A_6, $A_{6\text{End}}$, and A_7) overestimates the DPBR. The relative phase error for each method is much less than the magnitude error at frequencies less than 1000 Hz. The cap resonance in the range of 1300–1500 Hz greatly influences the DPBR values in both phase and magnitude evaluated using these full handle methods.

The handle base and the fixture are usually rigidly connected when the force sensor is located at the interface between the fixture and shaker armature for the total DPBR measurement (e.g. Ref. [16]). Therefore, the use of F_7 and the acceleration at the handle fixture (A_7) for the DPBR evaluation is equivalent to the use of F_6 and $A_{6\text{End}}$ if the fixture is sufficiently rigid. Similarly, the use of F_7 and A_6 is equivalent to the use of F_6 and A_6 for the evaluation. As in the use of F_6 and A_5, the use of F_7 and A_5 for the evaluation also generally underestimates the DPBR at the high frequencies.

The above results and analyses suggest that the best method for directly measuring the total DPBR is to use F_6 and A_6 for the evaluation. Therefore, further parametric studies were performed to identify the major factors affecting this method. Similar to the effects of K_5 and C_5 on the cap measurement method [4], the variations of K_6 and C_6 had little effect on the modeling results; variations of M_6 and M_7 also had little effect. Relaxing the cap and base connection (K_5 and C_5) reduced the resonant frequency and thus generally increased the error at a given frequency. The reduction of the cap mass reduced the error; this is also consistent with the prediction of Eqs. (7) and (9).

Similar to the effects of the inter-structure vibration variation, the first type of error induced by the handle bending motion stems from the fact that the measured vibration could not be the same as that input to the

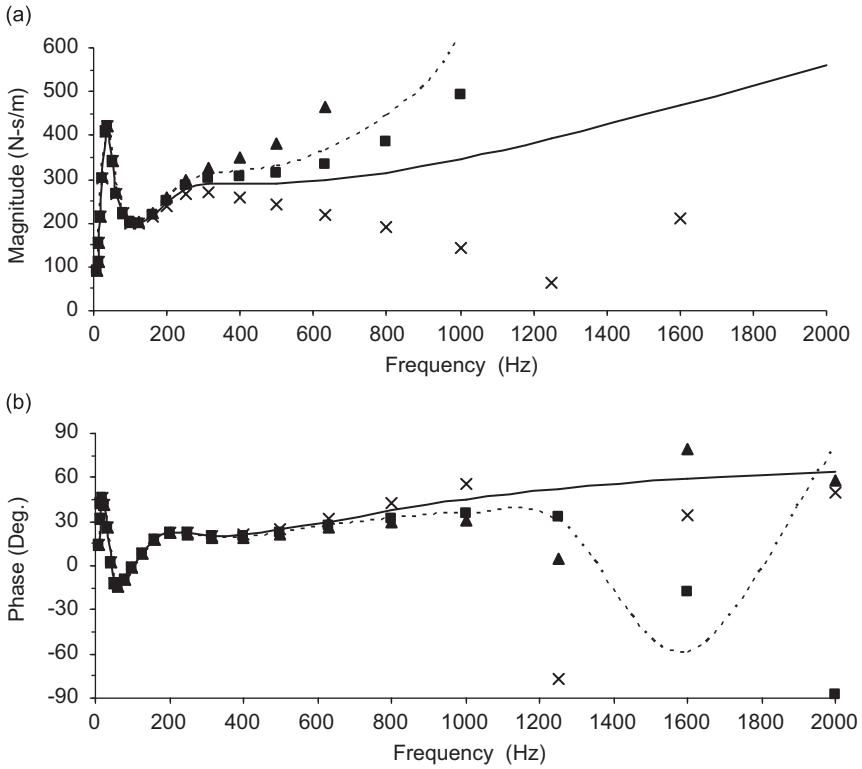

Fig. 13. Comparisons of accurate solution (_____) and hand mechanical impedance (a) magnitude and (b) phase angle calculated using F_6 and accelerations at three locations: ▲, acceleration on the handle fixture (A_7); ·····, acceleration at one end of the handle base (A_{6End}); ■, acceleration at the center of handle base (A_6); and ×, acceleration at the center of handle measuring cap (A_5).

hand. This effect was not simulated in the finite element modeling of the handle–hand–arm system but was examined using the analytical method. As shown in Fig. 7, a hand must cover a certain range of the handle on which the vibration is generally not uniformly distributed because of the bending motions. Whereas the force sensors can track the summation of the distributed forces, only one accelerometer is usually used to measure the vibration at a specific location on the handle. If the measured acceleration represents the maximum vibration on the handle, this study proves that the actual DPBR will be greater than the measured DPBR (see the detailed proof in Appendix A). This is what likely occurs in many cases, because the accelerometer is usually positioned at the handle center where the vibration reaches its maximum value, as shown in Fig. 9. This analytical prediction was verified in the finite element modeling by positioning a 20 g calibration mass on a 30 mm handle at three different locations: at a position on the cap end, at the position of the force sensor, and at the handle center. The parameters of the 30 mm handle are listed in Table 3. When the best full handle method was used, the corresponding errors on the cap were −6.0%, −6.7%, and −3.5%, respectively. On the handle base, the corresponding errors were −35.1%, −32.6, and −36.5%, respectively. The differences among the percent errors observed on each structure (cap or base) demonstrate that one of the error generation mechanisms is related to the response distribution effect. The percent errors on each structure also include the tare mass cancellation errors due to the influence of the hand coupling on the bending response of the structure, which is also clearly reflected in the analytical formulas presented in Appendix A.

The bending motion-induced error could exceed that induced by the uneven rigid body motion if the bending stiffness of the handle is greatly reduced. For example, the installation of the force sensors at the ends of the handle base for the DPBR measurement could reduce the end bending constraint and increase its bending motion. It is also common knowledge that reducing the handle diameter could greatly decrease the bending stiffness of both the cap and base, and that increasing the cap support span could largely reduce

Table 3
Additional parameters for the parametric studies

30 mm handle			
m_C (kg/m)	0.371	I_C (m^4)	4.717e−9
m_{B1} (kg/m)	0.617	I_{B1} (m^4)	5.059e−9
48 mm handle			
m_C (kg/m)	1.195	I_C (m^4)	4.400e−8
m_{B1} (kg/m)	1.894	I_{B1} (m^4)	5.740e−8
Meshing for all the three handles			
L_{c1} (m)	0.021	L_{c2} (m)	0.033
L_{b1} (m)	0.006	L_{b2} (m)	0.006
L_{b3} (m)	0.029	L_{b4} (m)	0.033

Note: If not mentioned in this table, the parameters required for the simulation are the same as those in Table 2.

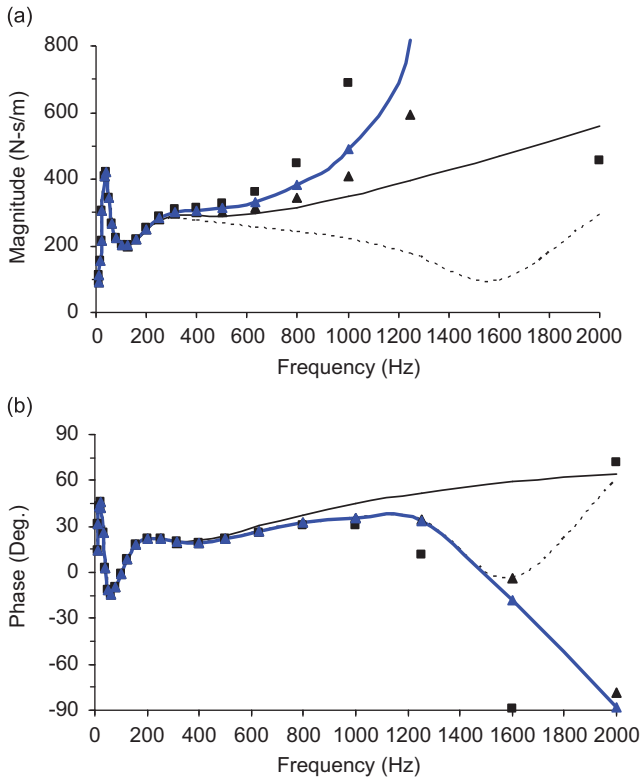

Fig. 14. The combined effect of handle diameter, end bending stiffness ($K_B = 1$ kN-m/Rad), and cap support span ($L_S = 66$ mm) on the impedance response: (a) magnitude and (b) phase angle (_____, accurate solution; ·····, 30 mm handle; ▲, 40 mm handle; —▲—, 40 mm handle with the baseline span and end bending stiffness listed in Table 2; ■, 48 mm handle).

the bending stiffness [20]. Fig. 14 shows the combined effect of these three factors on mechanical impedance. The additional parameters required in the simulation are also listed in Table 3. For a direct comparison, the DPBR simulated using the 40 mm handle baseline parameters is also plotted in this figure. As shown in figure, the increased bending motion due to the changes in the supporting spans and constraints on the 40 mm handle produced responses that are lower than the baseline data and closer to the accurate solution. However, a large underestimation of the DPBR was observed on the 30 mm handle.

4. Discussion

This study developed a model of the fixture–handle–hand–arm system and applied it to investigate errors in DPBR measurements that are induced by handle structure responses. Although the exact dynamic behaviors of the handle structure used in this study may be different than some of those used in many reported studies, the basic principles of the handle structure responses-induced errors are the same, and the error sources identified in this study may generally exist with many instrumented handles. Although only the rigid body and bending modes of the handle structure responses were considered in this study, the basic mechanisms of the measurement error generations for other types of structure responses (e.g., handle twisting and rotational motion) are similar, as demonstrated in the similarity between the rigid body motion effects and bending motion effects. Therefore, the principles identified in this study can be generally applied to evaluate the reliability and accuracy of various measurement methods and to identify the best approach to conduct the measurement and to improve it.

The basic principles are summarized as follows:

- The handle dynamics-induced error exists essentially because the vibration motion measured at one point on the handle (A_{Measured}) and used to evaluate the DPBR is not always the same as that at every other point, $A(x)$, in terms of both magnitude and phase angle. Simply put, $A(x) \neq A_{\text{Measured}}$.
- The variation of the vibration distribution generally results from three sources: (I) inter-structure vibration differences due to connection flexibility; (II) intra-structure vibration differences due to structure flexibility; and (III) the effects of hand coupling on the inter- and intra-structure vibration differences.
- There are two specific mechanisms involved in error generation: (i) the first type of error exists when the actual biodynamic response distributed at one point is different from that evaluated using the measured acceleration; and (ii) the second type of error is present whenever the tare mass measured without hand coupling is different from that included in the DPBR measurement.

4.1. Error sources of the cap measurement method

According to the principles, the most effective approach to reducing handle dynamics-induced errors is to minimize the number of structures directly involved in the DPBR measurement or to make the tare structure as simple, rigid, and light as possible. The cap measurement method applies this concept, which avoids the inter-structure effects and minimizes the intra-structure effects. Therefore, the systematic errors inherent with this method are minimal. Furthermore, the cap method makes it possible to measure the distributed biodynamic responses, which are essential to construct a more realistic model of the hand–arm system [5].

A major drawback of this method is that the responses distributed at the fingers and the palm cannot be simultaneously measured using the handle design shown in Fig. 2. This requires more experimental time. The experimental procedures also introduce an additional random factor in the measurement, which is that the hand may not couple to the handle in exactly the same manner in each trial. Markers placed on handle and hand can be used to help the grip alignment such that this random error can be reduced [8]. Increasing the number of measurement trials may also reduce this random effect. Alternatively, this drawback can be avoided by designing a handle with two measuring caps, which has been attempted by Welcome and Dong [22]. A problem with such a design is that the handle base is weakened. According to the modeling results of this study, such a change should have no significant effect on the DPBR measurement. However, the base bending motion may affect force sensor behavior that is not taken into account in this modeling. Further experimental studies are required to assess the feasibility of this improvement approach. Nevertheless, this drawback is not a critical problem to the cap method.

4.2. Error sources of the full handle measurement methods

The results of this study revealed that it is theoretically acceptable to use any of the reported methods to measure the total DPBR of the hand–arm system up to a certain frequency, and the useful frequency range

generally increases with the increase in the handle resonant frequency. However, at higher frequencies, none of the methods that directly measure the total DPBR of the entire hand–arm system using a split instrumented handle could provide an accurate measurement. Errors generally increase with the increase in frequency in the range of concern for hand-transmitted vibration exposure.

According to the first principle identified in this study, the measurement errors could be minimized if a sufficient number of accelerometers are installed on the handle. For example, Eq. (7) provides an approach to correct the error due to the inter-structures rigid body vibration difference. This may be achieved by simultaneously measuring the accelerations on both the cap and the base and using the transmissibility functions to correct the error. Furthermore, the additional accelerometer may also make it possible to simultaneously measure the total DPBR and those responses distributed at the fingers and the palm of the hand using the handle reported in Ref. [15], provided the error due to the handle bending can be ignored.

The results of this study also indicate that the uneven vibration distributions due to the flexibilities or the bending motions of the handle base and cap are other important sources of error associated with the full handle method. Because the span of the handle base is larger than that of the cap, and the fact that the palm is generally positioned in the middle range of the base, the base bending effect is generally larger than that observed with the cap measurement method, as observed in this study. Similar to the rigid body effects, the intra-structure responses-induced errors also resulted from both the difference itself and the hand coupling's influence on the difference. Similar to the cap method, the intra-structure response generally tends to underestimate the DPBR except at the ends of the cap, which is opposite of the rigid body motion effects. Whether the DPBR is overestimated or underestimated depends on the specific handle structure properties or which type of effect plays the dominant role in the measurement. As observed in this study, many structural factors could affect these two types of motions. Various studies have reported different instrumented handle structures. The stiffness and damping values of the force sensors used in these studies could also be different. Therefore, these handles may exhibit very different dynamic characteristics. As a result, a portion of them may overestimate the DPBR, while others could underestimate it. Furthermore, many of the reported studies used acceleration values measured at different locations for the DPBR evaluation. As found in this study, this could also result in large differences in DPBR measurements. These observations at least partially explain why the reported DPBRs at high frequencies could be very different [9,10].

The results of this study also indicate that the useful frequency range of the full handle measurement methods depends on the handle's fundamental resonant frequency. The fundamental resonance frequency of the handle used in this study is 1452 Hz. If data with errors larger than 10% are considered unacceptable, this handle can only be used for response measurements below 500 Hz, which is approximately one-third of the resonant frequency. As found in an experimental study [8], it is very difficult to increase the fundamental resonance of the fixture–handle system beyond 2000 Hz. Therefore, it is very difficult to use such a handle to obtain a reliable and accurate measurement of the DPBR at high frequencies using the full handle methods.

Marcotte and his colleagues [15] experimentally investigated the effect of handle diameter (30, 40, and 50 mm) on the total DPBR using an instrumented handle similar to that used in the current study. In that study, two additional force sensors were installed at the handle base-fixture interface. They reported that reducing the handle diameter reduced the DPBR at high frequencies (>100 Hz). At 1000 Hz, the DPBR measured on the 40 mm handle was about two times that measured with the 30 mm handle. Coincidently, as shown in Fig. 14, the reduction of the handle diameter could also underestimate the DPBR. It is unclear whether the reported experimental data include the systematic error due to the bending motion effect, or the DPBR really displays such a characteristic, or the data included both factors. Further studies are required to clarify this.

The measurement method developed by Lundström and Burström [10] has some similarities to the cap measurement method developed by Dong et al. [4]. If the cap and base beam of their instrumented handle is sufficiently rigidly connected, the force measurement may directly track the response of the cap-beam assembly. If the two cap-beam assemblies are sufficiently symmetrical, the motion measured on one of the assemblies may be representative of that on the other. Under such conditions, the assemblies' bending effects become the major potential error source for this handle's results. These errors may be minimized by enhancing the stiffness of the cap-beam assembly. The most critical issue with this handle is whether the dynamic force could be reliably and accurately measured using the beams equipped with the strain gauges, as evidenced when

the strain gauges were replaced with two force sensors installed at the handle–fixture interface in their later version of the handle [17]. If the strain gauge method can provide reliable and accurate dynamic force measurements, the gauge circuit can be modified to simultaneously measure the DPBRs distributed at the fingers and the palm of the hand.

4.3. Operational calibration test

This modeling study did not take into account some influencing factors that could also significantly affect the experimental data. These factors may include the sensor accuracy and reliability, the effect of the structure responses on the sensor behaviors, and the deficiencies and/or inaccuracy of the handle model and material properties. If the mounting of the accelerometer to the handle lacks rigidity, the measured acceleration could result in DPBR underestimations, similar to the effect when using the acceleration on the cap in the full handle method or evaluated using F_6 and A_5, as shown in Fig. 12 or Eq. (9). These errors may be detected by performing the operational calibration test. The results of this study also suggest that the errors due to hand dynamics can also be detected using such a test. The operational calibration test may also be used to correct at least a portion of the overall errors.

5. Conclusions

This study establishes that major systematic errors in DPBR measurements may result from handle structure dynamics. The essential reason for the errors is that the vibration motion measured at one point on the handle and used for the DPBR evaluation is not always the same as that at every other location. The variation of the vibration distribution generally results from three sources: (I) inter-structure vibration differences due to connection flexibility; (II) intra-structure vibration differences due to structure flexibility and/or rotational rigid body motions; and (III) the effects of hand coupling on the inter- and intra-structure vibration differences. There are two mechanisms involved in the error generation: (i) the uneven vibration distribution-induced error appears when the actual biodynamic response distributed at a point is different from that evaluated using the measured acceleration; and (ii) the tare mass cancellation error is present when the tare mass values measured with and without hand coupling are different.

The three sources of vibration variation generally exist in the full handle method using a split instrumented handle. The DPBR measured using this method could overestimate or underestimate the high frequency DPBR, mainly depending on the fundamental resonance of the handle and the specific locations at which the dynamic force and vibration are measured for the DPBR evaluation. The full handle method may be suitable for the DPBR measurement at frequencies less than one-third of the handle's fundamental resonant frequency.

The cap measurement method avoids the inter-structure vibration variation and its related hand coupling effect. To minimize intra-structure errors, the cap assembly can be made sufficiently small and rigid, and the force sensors can be positioned at the nodes of the first bending mode. The results of this study demonstrate that the systematic errors inherent with the cap method are minimal. Therefore, it is the best one among the DPBR measurement methods examined in this study.

The modeling study also theoretically proves that the response of the entire hand–arm system can be obtained from the vector summation of the distributed responses. The results of this study also suggest that the optional handle calibration test using a mass rigidly and separately attached to various locations on the handle tare structure(s) is a practical and effective approach to examine the overall reliability and accuracy of the DPBR measurement system.

Disclaimers

The content of this publication does not necessarily reflect the views or policies of the National Institute for Occupational Safety and Health (NIOSH), nor does mention of trade names, commercial products, or organizations imply endorsement by the US Government.

Appendix A. Derivations of the analytical formulas for predicting the biodynamic response

A.1. Rigid body motion solutions

When the measuring cap is considered a rigid body (M_5), an analytical solution for each measurement method can be obtained. With the typical cap measurement method [4], the DPBR (M_{55}) is evaluated using the acceleration measured on the measuring cap (A_5) and the dynamic force (F_5) measured on the two force sensors that are represented using K_5 and C_5 in the model shown in Fig. 5. With this method, the finger DPBR (M_{Fingers}) expressed in Eq. (5) can be written as follows:

$$\begin{aligned} M_{55} &= F_{5\_\text{Coupled}}/A_{5\_\text{Coupled}} - M_5 = (F_4 + M_4 A_{5\_\text{Coupled}} + M_5 A_{5\_\text{Coupled}})/A_{5\_\text{Coupled}} - M_5 \\ &= F_4/A_{5\_\text{Coupled}} + M_4, \end{aligned} \tag{A.1}$$

where "Coupled" refers to measurement with the hand coupled to the handle. Using the formula in Eq. (1) and considering that $A_{\text{Fingers}} = A_{5\_\text{Coupled}}$, we prove that

$$M_{55} = F_4/A_{\text{Fingers}} + M_4 = M_{\text{Fingers}}. \tag{A.2}$$

Similarly, when the palm is positioned on the measuring cap, the cap method for the palm DPBR (M_{Palm}) can be expressed as follows:

$$M_{55} = M_{\text{Palm}}. \tag{A.3}$$

When the handle base is also considered a rigid body (M_6), the formula for calculating the DPBR of the entire hand–arm system with a full handle method can also be derived from the model shown in Fig. 5, together with Eqs. (1) and (6). For example, the full handle method with the use of F_6 (represented using K_6 and C_6) and A_6 (acceleration on the handle base) for evaluating DPBR (M_{66}) can be expressed as follows:

$$\begin{aligned} M_{66} &= F_{6\_\text{Coupled}}/A_{6\_\text{Coupled}} - F_{6\_\text{Uncoupled}}/A_{6\_\text{Uncoupled}} = (F_3 + M_3 A_{6\_\text{coupled}} + M_6 A_{6\_\text{Coupled}} \\ &\quad + F_4 + M_4 A_{5\_\text{coupled}} + M_5 A_{5\_\text{Coupled}})/A_{6\_\text{Coupled}} - (M_6 A_{6\_\text{Uncoupled}} + M_5 A_{5\_\text{Uncoupled}})/A_{6\_\text{Uncoupled}} \\ &= M_{\text{Palm}} + \alpha M_{\text{Fingers}} + (\alpha - \beta) M_5 \neq M_{\text{Hand}}, \end{aligned} \tag{A.4}$$

where

$$\begin{aligned} \alpha &= A_{5\_\text{Coupled}}/A_{6\_\text{Coupled}}, \\ \beta &= A_{5\_\text{Uncoupled}}/A_{6\_\text{Uncoupled}}, \end{aligned} \tag{A.5}$$

where "Uncoupled" refers to the measurement without hand coupling or the measurement of the handle tare response.

Similarly, the full handle method with the use of F_6 and A_5 (acceleration on the handle cap) for evaluating DPBR (M_{65}) can be expressed as follows:

$$M_{65} = M_{\text{Fingers}} + \frac{1}{\alpha} M_{\text{Palm}} + \left(\frac{1}{\alpha} - \frac{1}{\beta}\right) M_6 \neq M_{\text{Hand}}. \tag{A.6}$$

Eqs. (A.4) and (A.6) indicate that there are two types of errors. The first one is related to the distributed biodynamic response (M_{Fingers} or M_{Palm}) and the second one is related to the tare mass (M_5 or M_6).

A.2. Bending motion solutions

Similar to the case of the rigid body vibration variation, the first type of error is also due to the uneven distribution of the vibration on each handle structure. With the distributed biodynamic forces conceptually

illustrated in Fig. 7, the measured biodynamic response (M_{Measured}) can be expressed as follows:

$$M_{\text{Measured}} = \frac{F}{A_{\text{Measured\_Coupled}}} = \int_L \frac{\mathrm{d}F(x)}{A_{\text{Measured\_Coupled}}} = \int_L \frac{A_{\text{Coupled}}(x)}{A_{\text{Measured\_Coupled}}} \frac{\mathrm{d}F(x)}{A_{\text{Coupled}}(x)}$$
$$= \int_L \frac{1}{\eta(x)}\,\mathrm{d}M(x) \neq \int_L \mathrm{d}M(x) = M_{\text{Actual}}, \tag{A.7}$$

where F is the measured biodynamic force, A_{Measured} is the measured acceleration, $A(x)$ is the acceleration located at x, M_{Actual} is the summation of the distributed biodynamic response ($\mathrm{d}M$), and

$$\eta(x) = A_{\text{Measured\_Coupled}}/A_{\text{Coupled}}(x). \tag{A.8}$$

If the acceleration is measured at the location with the maximum value, and the phase differences among the distributed accelerations are not significant, Eqs. (A.5) and (A.6) suggest that

$$\eta \geqslant 1 \quad \text{and} \quad M_{\text{Actural}} > M_{\text{Measured}}. \tag{A.9}$$

Also similar to the case of the rigid body vibration variation, the second type of error for the intra-structure vibration variation also results from the hand coupling effect on the tare mass cancellation. Hand coupling can change the vibration distribution, but it cannot change the mass value at each point of each structure, which can be expressed as follows:

$$\mathrm{d}M_{\text{Coupled}}(x) = \frac{\mathrm{d}F_{\text{Handle\_Coupled}}(x)}{A_{\text{Coupled}}(x)} = \frac{\mathrm{d}F_{\text{Handle\_Uncoupled}}(x)}{A_{\text{Uncoupled}}(x)} = \mathrm{d}M_{\text{Uncoupled}}(x), \tag{A.10}$$

However, the measured tare mass could be different from the actual mass because there is generally a difference between the actual and measured accelerations. The residual of the mass cancellation (ΔM_{Tare}) can be estimated from:

$$\Delta M_{\text{Tare}} = M_{\text{Coupled\_Tare}} - M_{\text{Uncoupled\_Tare}} = \int_L \frac{\mathrm{d}F_{\text{Handle\_Coupled}}}{A_{\text{Measured\_Coupled}}} - \int_L \frac{\mathrm{d}F_{\text{Handle\_Uncoupled}}}{A_{\text{Measured\_Uncoupled}}}$$
$$= \int_L \frac{1}{\eta(x)} \frac{\mathrm{d}F_{\text{Handle\_Coupled}}}{A_{\text{Coupled}}(x)} - \int_L \frac{1}{\lambda(x)} \frac{\mathrm{d}F_{\text{Handle\_Uncoupled}}}{A_{\text{Uncoupled}}(x)} = \int_L \left[\frac{1}{\eta(x)} - \frac{1}{\lambda(x)}\right] \mathrm{d}M_{\text{Handle}} \neq 0, \tag{A.11}$$

where

$$\lambda(x) = A_{\text{Measured\_Uncoupled}}/A_{\text{Uncoupled}}(x). \tag{A.12}$$

If the measured bending component of the acceleration with hand coupling is greater than that without hand coupling, and their phase difference is not significant, Eqs. (A.6), (A.9) and (A.10) suggest that

$$\eta \geqslant \lambda, \quad \Delta M_{\text{Tare}} < 0, \quad M_{\text{Actual}} > M_{\text{Measured}} \tag{A.13}$$

A.3. Combined rigid body and bending motion solutions

The separate solutions can be used to form the combined solution by superposition. For example, using Eqs. (A.2) and (A.5), the finger DPBR evaluated with the typical cap method can be expressed as follows:

$$M_{\text{Finger\_Measured}} = \int_L \frac{1}{\eta_{\text{Cap}}}\,\mathrm{d}M_{\text{Fingers}} + \int_L \left[\frac{1}{\eta_{\text{Cap}}} - \frac{1}{\lambda_{\text{Cap}}}\right] \mathrm{d}M_{\text{Fingers}} \neq M_{\text{Finger\_Actual}}. \tag{A.14}$$

Using Eqs. (A.4), (A.5), and (A.9), the hand DPBR evaluated with the typical full handle method can be expressed as follows:

$$M_{\text{Hand\_Measured}} = \int_L \frac{1}{\eta_{\text{Base}}}\,\mathrm{d}M_{\text{Palm}} + \int_L \left[\frac{1}{\eta_{\text{Base}}} - \frac{1}{\lambda_{\text{Base}}}\right]\mathrm{d}M_{\text{Base}} + \alpha\int_L \frac{1}{\eta_{\text{Cap}}}\,\mathrm{d}M_{\text{Fingers}} + \left[\alpha\int_L \frac{1}{\eta_{\text{Cap}}}\,\mathrm{d}M_{\text{Cap}} - \beta\int_L \frac{1}{\lambda_{\text{Cap}}}\,\mathrm{d}M_{\text{Cap}}\right] \neq M_{\text{Hand\_Actual}}. \tag{A.15}$$

References

[1] M.J. Griffin, Foundations of hand-transmitted vibration standards, *Nagoya Journal of Medical Science* 57 (supplement) (1994) 147–164.

[2] R.G. Dong, J.Z. Wu, D.E. Welcome, Recent advances in biodynamics of hand–arm system, *Industrial Health* 43 (3) (2005) 449–471.

[3] ISO 5349-1, *Mechanical Vibration—Measurement and Evaluation of Human Exposure to Hand-Transmitted Vibration—Part 1: General Guidelines*, International Organization of Standard, Geneva, Switzerland, 2001.

[4] R.G. Dong, J.Z. Wu, T.W. McDowell, D.E. Welcome, A.W. Schopper, Distribution of mechanical impedance at the fingers and the palm of human hand, *Journal of Biomechanics* 38 (5) (2005) 1165–1175.

[5] R.G. Dong, J.H. Dong, J.Z. Wu, S. Rakheja, Modeling of biodynamic responses distributed at the fingers and the palm of the human hand–arm system, *Journal of Biomechanics* 40 (10) (2007) 2335–2340.

[6] J.H. Dong, R.G. Dong, S. Rakheja, D.E. Welcome, T.W. McDowell, J.Z. Wu, A method for analyzing absorbed power distribution in the hand and arm substructures when operating vibrating tools, *Journal of Sound and Vibration* 311 (3–5) (2008) 1286–1309.

[7] T.W. McDowell, M.L. Kashon, D.E. Welcome, C. Warren, R.G. Dong, Relationships between psychometrics, exposure conditions, and vibration power absorption in the hand–arm system, *Proceedings of the 11th International Conference on Hand– Arm Vibration*, Bologna, Italy, 2007, pp. 417–424.

[8] R.G. Dong, D.E. Welcome, T.W. McDowell, J.Z. Wu, Measurement of biodynamic response of human hand–arm system, *Journal of Sound and Vibration* 294 (4–5) (2006) 807–827.

[9] R. Gurram, S. Rakheja, A.J. Brammer, Driving-point mechanical impedance of the human hand–arm system: synthesis and model development, *Journal of Sound and Vibration* 180 (3) (1995) 437–458.

[10] R. Lundström, L. Burström, Mechanical impedance of the human hand–arm system, *International Journal of Industrial Ergonomics* 3 (3) (1989) 235–242.

[11] SO 10068, *Mechanical Vibration and Shock-Free, Mechanical Impedance of the Human Hand– Arm System at the Driving Point*, International Organization for Standardization, Geneva, Switzerland, 1998.

[12] R.G. Dong, D.E. Welcome, J.Z. Wu, T.W. McDowell, Development of hand–arm system models for vibrating tool analysis and test rig construction, *Noise Control Engineering Journal* 56 (1) (2008) 35–44.

[13] T. Miwa, Studies on hand protectors for portable vibration tools, *Industrial Health* 2 (2) (1964) 95–105.

[14] A.J. Besa, F.J. Valero, J.L. Suñer, J. Carballeira, Characterisation of the mechanical impedance of the human hand–arm system: the influence of vibration direction, hand–arm posture and muscle tension, *International Journal of Industrial Ergonomics* 37 (3) (2007) 225–231.

[15] P. Marcotte, Y. Aldien, P.E. Boileau, S. Rakheja, J. Boutin, Effect of handle size and hand–handle contact force on the biodynamic response of the hand–arm system under z_h-axis vibration, *Journal of Sound and Vibration* 283 (3–5) (2005) 1071–1091.

[16] D.D. Reynolds, R.J. Falkenberg, A study of hand vibration on chipping and grinding operators, part II: four-degree-of-freedom lumped parameter model of the vibration response of the human hand, *Journal of Sound and Vibration* 95 (4) (1984) 499–514.

[17] L. Burström, Measurements of the impedance of the hand and arm, *International Archives of Occupational Environment and Health* 62 (6) (1990) 431–439.

[18] P. Marcotte, S. Adewusi, J. Boutin, H. Nelisse, S. Rakheja, P.E. Boileau, Modeling the contributions of handle dynamics on the biodynamic response of the human hand–arm system, *Proceedings of the 11th International Conference on Hand– Arm Vibration*, Bologna, Italy, 2007, pp. 321–326.

[19] R.G. Dong, D.E. Welcome, T.W. McDowell, J.Z. Wu, How to accurately measure the biodynamic responses of the hand–arm system, *Proceedings of the 11th International Conference on Hand– Arm Vibration*, Bologna, Italy, 2007, pp. 311–320.

[20] D.G. Fertis, *Mechanical and Structure Vibrations*, Wiley, New York, 1995.

[21] E. Ogberg, *Machinery's Handbook*, 26th ed., Industrial Press Inc., New York, 2000.

[22] D.E. Welcome, R.G. Dong, Instrumented handles for studying hand-transmitted vibration exposure, *Proceedings of the First American Conference on Human Vibration*, Morgantown, WV, 2006, pp. 140–141.